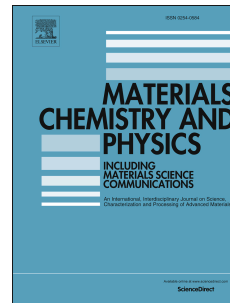


Accepted Manuscript

Fcc→bcc→hcp successive phase transformations in the strained ultrathin copper film:
A molecular dynamic simulation study

Bin Sun, Wenze Ouyang, Jijiang Ren, Liwei Mi, Wei Guo



PII: S0254-0584(18)30796-X

DOI: [10.1016/j.matchemphys.2018.09.045](https://doi.org/10.1016/j.matchemphys.2018.09.045)

Reference: MAC 20974

To appear in: *Materials Chemistry and Physics*

Received Date: 28 August 2017

Revised Date: 9 June 2018

Accepted Date: 10 September 2018

Please cite this article as: Bin Sun, Wenze Ouyang, Jijiang Ren, Liwei Mi, Wei Guo, Fcc→bcc→hcp successive phase transformations in the strained ultrathin copper film: A molecular dynamic simulation study, *Materials Chemistry and Physics* (2018), doi: 10.1016/j.matchemphys.2018.09.045

This is a PDF file of an unedited manuscript that has been accepted for publication. As a service to our customers we are providing this early version of the manuscript. The manuscript will undergo copyediting, typesetting, and review of the resulting proof before it is published in its final form. Please note that during the production process errors may be discovered which could affect the content, and all legal disclaimers that apply to the journal pertain.

Fcc→bcc→hcp successive phase transformations in the strained ultrathin copper film: A molecular dynamic simulation study

Bin Sun^{*a}, Wenze Ouyang^{*b}, Jijiang Ren^c, Liwei Mi^a, Wei Guo^a,

^a*School of Materials and Chemical Engineering, Zhongyuan University of Technology, Zhengzhou 450007, People's Republic of China. E-mail: sunbin7610@sina.com, Fax: +86 37162499997*

^b*Key Laboratory of Microgravity (National Microgravity Laboratory), Institute of Mechanics, Chinese Academy of Sciences, Beijing 100190, People's Republic of China. E-mail: oywz@imech.ac.cn, Fax: +86 1082544096; Tel: +86 1082544099*

^c*School of Textiles, Zhongyuan University of Technology, Zhengzhou 450007, People's Republic of China*

Abstract: The phase transformation behaviors of ultrathin Cu film under uniaxial tensile stress are investigated using molecular dynamic simulation. With the stress increasing, Cu film undergoes a successive phase transformation, i.e. firstly fcc→bcc, then bcc→hcp. The phase transformation process is very fast and thorough, i.e., all parents phase can transit into the new phase almost instantaneously. The crystallography mechanisms of two martensitic transformations are exactly corresponding to Bain and Burgers mechanism, respectively. By examining the formation conditions of such phase transformation in Cu film, we reveal that this fcc→bcc→hcp successive phase transformation will be subject to the very strict simulation conditions, namely stretching along [100] (or [010], [001]) direction, definitive tensile speed (1×10^{10} /s), appropriate film thickness (0.7230 -18.08 nm), low temperature ($T \leq 10$ K), and continuous stretching process without any relaxation procedure.

Keywords: Phase transformation, Nanometer Cu film, Uniaxial tensile strain, Molecular dynamic simulation

0 Introduction

Nanometer-scale-thick metallic films are widely used in modern technologies such as the microelectronics and nanofabrication[1,2]. For a safe and reliable design of such systems, it is very important to understand the mechanical behaviors of the films under the deformation. For the nano-films or nanowires of many metals, e.g. Fe, Ni, Co, etc, the martensitic phase transformation is often observed during the deformation process (tension or compression) [3-8]. A martensitic transformation is a stress-driven diffusionless structural phase transition that occurs through collective atomic motion[9,10]. For example, some pioneering experiments discovered that the iron underwent a stress-induced martensitic phase transformation where the ground state crystal structure of body-centered cubic (bcc) transformed into a hexagonal close-packed (hcp) structure[11]. Within a certain range of pressure and temperature, bcc iron was also found to transform into a reversible face-centered cubic (fcc) structure[12-14].

The martensitic phase transformation of Cu has attracted great attention in the past two decades owing to the experimental observations that some higher-energy phases of Cu (bcc and hcp Cu) existed in the pseudomorphic Cu films grown on the {001} surface of Pd[15], Pt[16], Ag[17], and Fe[18,19] and in multilayers of Cu with Nb [20, 21]. The lattice structure of fcc is the ground state of Cu while bcc or hcp is considered to be unstable based on first-principles total energy calculations[22, 23]. Wang and Sob et al.[24] studied the phase transformation modes in Cu, finding that its higher energy phases (bcc Cu and 9R Cu[24]) can be stabilized in the region of extended defects by certain imposed constrains. Jona and Marcus et al. [25] had also proved by vacuum deposition of Cu on W{001} that the hcp Cu is stable in small regions, even in surprising thick films. Mishin et al.[23] used the embedded-atom method (EAM) potentials to calculate the structural stability of different phases in Cu, indicating that the bcc structure of Cu is elastically unstable, while the hcp or 9R structure of Cu are metastable. Additionally, molecular dynamic (MD) simulation is employed to study the dynamics of structural phase transition and the path. Kolluri et

al. [26] investigated the dynamic process of fcc→hcp phase transformation in biaxially strained thin film of Cu, indicating that martensitic transformations nucleate heterogeneously at the film's surface and subsequently grow into the bulk, and that the growth process is mediated by the propagation of stacking faults. S. Tang et al. [27] studied the multistep nucleation process of fcc crystals from non-equilibrium liquid using phase-field crystal simulations. It was elucidated that bcc precursors provide a 'substrate' for formation of fcc nuclei, i.e. [112] surfaces and steps on [110] surfaces of bcc precursors serve as energetically favorable sites for fcc nucleation.

Despite lots of effort have been paid to explore the mechanisms of the martensitic transformation of Cu[15-26], a fundamental and complete understanding remains elusive. For instance, the existence of the bcc or hcp Cu phase needs to be verified. Even if the bcc or hcp phase does exist, its decisive factors and the exact paths of fcc→bcc or bcc→hcp phase transformation are not clear yet. In 2017, A. Neogi and N. Mitra [28, 29] discovered the phase transformation behavior induced by shock compression of single crystal Cu via classical MD simulations as well as *ab-initio* MD simulations. They found that during shock wave propagation along [100] and [110], a fcc-to-bcc phase transformation has been observed to occur behind the shock front at higher intensity of shock (piston velocity > 1.5 km/s). Three different local lattice structure identification methods had been utilized to confirm such structural phase transformation.

To further understand the structural transition and predict the mechanical behaviors of Cu thin films, we perform molecular dynamic (MD) simulations to study the phase transformation of ultrathin (~ a nanometer) Cu film that has been strained uniaxially along [100] direction. Interestingly the structure of Cu film, with the stress increasing, goes through successive phase transformations, i.e. firstly fcc→bcc, then bcc→hcp. Moreover, these phase transformations are thorough and rapid, namely the whole Cu film with fcc structure completely transits into the one with bcc structure, then into the one with hcp structure in a very short time. To the best of our knowledge, it is the first time in computer simulation to observe the fcc→bcc→hcp successive phase transformation of Cu film under stretching stress. The mechanisms and formation

conditions of such phase transformation are discussed in detail. We expect that this work helps to understand theoretically the mechanism of martensitic transformation, as well as to provide the experiments with a guide in the search for possible metastable phases.

1 Details of molecular dynamics simulation

The simulated system is a Cu film with dimension of $50a_0 \times 30a_0 \times 3a_0$ (a_0 is the lattice constant of fcc Cu, $a_0 = 0.3615$ nm), and it contains $N = 18,000$ atoms. We orient x axis along the $[100]$ direction, y axis along the $[010]$ direction, and z axis along the $[001]$ direction. Periodic boundary conditions are adopted in all directions, and the temperature T is kept at 10K during the whole simulation process to avoid thermal activation. In the beginning of the simulation, the system of Cu film is relaxed for 50 ps to minimize the potential energy of system. Then a uniaxial tension with a constant strain rate ($1 \times 10^{10}/s$) is loaded along the x direction until the total strain reaches 60%. It is noted that the simulation of uniaxial tension is continuous without any relax procedure during stretching process. All the simulations are performed in the isobaric-isothermal (NPT) ensemble with a stress-free condition along y and z directions, and the time step is 1 fs. MD simulations are accomplished by solving the equations of motion, which is a combination of a Nöse-Hoover thermostat and a Parrinello-Rahman barostat[30]. The system stress is calculated using the virial definition without the kinetic portion [31], as used in previous MD simulations [32-33].

Molecular dynamics simulations have been carried out in Large scale Atomic/Molecular Massively Parallel Simulator (LAMMPS) package developed by Plimpton [34] at Sandia National Laboratories. The potential of Mishin's embedded atom method (EAM) [25] for Cu has been chosen in the present investigation to describe the interaction between Cu atoms. This potential is widely used to study the mechanical properties and associated deformation mechanisms in Cu nanowires/nanopillars[35]. After such MD simulations, Ovito software [36] is used for visualizing the evolution of the atomic structure, and the local structure around

each atom is resolved by using the common neighbor analysis (CNA) technique[37].

2 Results and discussion

Figure 1 (a) shows the evolution of the phase transformation of Cu film with the increasing of applied strain ε . The percentages of different lattice structures are plotted as the strain increases. Due to overlap of curves, the two insets in Figure 1(a) show the variations of percentages of different lattice structures in details. It can be seen that when the strain is less than 10%, the film keeps the perfect fcc structure. Once the strain is more than 10%, the percentage of fcc phase decreases rapidly, while the bcc structure increases sharply. When the strain reaches 11%, the whole Cu film completely transits into bcc phase structure. However, the bcc phase only exists in a narrow range of strain ε , for it instantly disappears and the second phase transformation bcc \rightarrow hcp takes place when ε reaches 14%. Until the strain reaches 32%, the percentage of the hcp phase begins to decrease, and the fcc and bcc phases emerge again, thus resulting in a mixture of fcc, bcc and hcp structure. In the final stretching stage, the fcc phase is dominant over the other two phases.

The variation of the stress during phase transformation is shown in Figure 1(b). Combining with Figure 1(a), we can see clearly that the stress in the film along the x direction changes significantly when the phase transformations occur. At first, the stress increases almost linearly with the strain when $\varepsilon < 9.5\%$ due to elastic deformation. Then the stress begins to drop instantly until it becomes zero at $\varepsilon = 11.2\%$ where the fcc \rightarrow bcc phase transformation exactly takes place. When $\varepsilon = 11.2\% - 13.6\%$, the stress is approximately equal to zero. During this stage, the Cu film have complete bcc phase structure. When the second phase transformation of bcc \rightarrow hcp occurs, the stress continues to decrease until it becomes negative. During the following stretching process($\varepsilon = 14.4\% - 15.2\%$), the hcp phase begins to form, and the stress raises linearly with the increasing of ε . When the strain reaches 15.2%, the stress once again becomes zero, and the whole Cu film transits into hcp phase structure completely. When the strain exceeds 32%, the Cu film becomes a mixed structure of fcc+bcc+hcp and correspondingly the stress once again decreases rapidly.

Meanwhile we also plot the volume of the film versus the strain in Figure 1(c). This curve is similar to that of the pressure since the pressure is regulated by volume change in *NPT* ensemble[30]. The variations of stress and volume shown in Figure 1(b) and 1(c) provide an indirect evidence that the phase transformations indeed take place in the course of Cu film stretching. As is known, there would be change in the volume during the martensitic transformation because of the variation of lattice type and lattice constant, and the stress, as the driving force of phase transformation, will also change accordingly[38, 39].

In the 1980s, Milstein and Farber [40] used theoretical arguments to show that, for a fcc crystal homogeneously deformed under a strict [100] uniaxial tensile load, a path of minimum energy takes the crystal into an unstressed bcc configuration via the bifurcation path. But from the viewpoint of dynamic stability, many theoretical studies had suggested that bcc structure of Cu represented an unstable state in which the bulk modulus $C' [(C_{11}-C_{22})/2]$ vanished or was even negative[23, 41-43]. Thus, the bcc structure in the bulk of pure Cu has not been found under common conditions. Even in computer simulation studies on the Cu film deformation (compression or stretching), unitary and complete bcc phase of Cu is rarely observed. For instance, the simulation investigation on shock compression of single crystal Cu, performed by A. Neogi and N. Mitra[28, 29], had elucidated that the maximum volume fraction of bcc lattice configuration of single crystal Cu can only reach 85% at 1.8 km/s shock intensity in [100] direction. The phase transformation of fcc→hcp is usually found to occur in Cu stretching since hcp structure of Cu is regarded as a metastable state[23-26, 44], namely a state that can be in local mechanical equilibrium but is not that of the lowest Gibbs free energy.

In the present work, we observed this novel phenomenon that the fcc→bcc→hcp successive phase transformation takes place during the ultrathin Cu film stretching. Furthermore, this phase transformation process is very fast and thorough (see Fig. 1(a)), i.e., all parents phase can change into the new phase almost instantaneously. All of those interesting results indicate that the simulation system used in our study is distinctive, which provides an ideal model for investigating the exact path of

martensitic phase transformation in Cu film and determining the decisive factors in forming these higher-energy phases.

In the previous researches on martensitic phase transformations occurring during metallic solidification, the crystallography mechanisms of fcc→bcc and bcc→hcp were studied extensively[23,40,45,46] to present a detailed process of crystal structure transition and to reveal the physical fundamentals of phase transformation. Among those theories, Bain mechanism and Burgers mechanism had been proved to be classical theories for describing the phase transformations process of fcc→bcc and bcc→hcp, respectively[47-49]. In term of these two mechanisms, the crystal structure transitions are accomplished by the shortest and simplest movement of atoms. In order to examine whether the phase transformations appearing in our work are corresponding to Bain mechanism and Burgers mechanism, we select some adjacent atoms as tracer atoms [37] to observe microstructural evolution of the lattice and the distance evolutions between atoms.

Firstly, the crystallography mechanism of fcc→bcc is studied. Figure 2 shows the microstructural evolution of the lattice and the distance evolutions between the adjacent atoms. Under the tensile force in the [100] direction, all atoms in the lattice slide not only along the stretching direction [100], but also along the shear direction [010]. Interestingly, when the strain reaches 10% (Fig. 2(c)), the lattice begins to deform by stretching in the [001] direction and compressing in the [010] direction. When the strain is 12.4%, this lattice deformation is more severe. The deformation of the lattice can be clearly verified by the variation of D_{1-3} , D_{2-4} and D_{2-11} in the Figure 2(e). In the case of not stretching, D_{1-3} , D_{2-4} and D_{2-11} are approximately equal to the lattice constant of fcc Cu ($a_{0, fcc} = 0.3615$ nm). As the strain increases, D_{1-3} begins to increase slightly since the direction of D_{1-3} is just in the stretching direction, and D_{2-4} and D_{2-11} reduced slightly. When the strain reaches 9.4%, D_{2-4} and D_{2-11} begin to change significantly, i.e., D_{2-4} decreases rapidly while D_{2-11} increases rapidly. When the strain reaches 12.4%, D_{1-3} and D_{2-11} have the same values of 0.406 nm, and D_{2-4} decreases to 0.286 nm.

Based on the evolutions of distance between atoms, we can see clearly that the

initial fcc structure has completely transitioned into bcc structure with the lattice constant of 0.286 nm when $\varepsilon = 12.4\%$. The lattice constant of bcc Cu presented here precisely agrees with the results reported by the literatures [50, 51] in which equilibrium lattice constant of bcc Cu was obtained by first-principles density-functional calculation. The path of phase transformation is also consistent with the classic Bain martensitic transformation theory, in which crystal structure transition results from lattice compressing in one direction and stretching in a vertical direction [48]. By calculation, the size of initial fcc lattice increases by 12% in the [001] and [100] directions and decreases by 21% in the [010] direction after the phase transformation of fcc \rightarrow bcc.

Microstructural evolutions of bcc \rightarrow hcp are shown in Figure 3, in which 17 atoms are selected as tracer atoms to observe the changes of atoms configuration with the strain increasing. Figure 3(a) - (d) display the atoms configuration in bcc lattice ($\varepsilon = 12.4\%$) and in hcp lattice ($\varepsilon = 22.0\%$) from the view of [010] direction and [100] direction, respectively. By comparing Figure 3(a) and 3(b), we find that as the strain increases the atoms in the middle layer (i.e., atoms of 10, 11 and 12) move towards the [001] direction, while the left atom layer (i.e., atoms of 1, 2, 13, 14, 15, 16 and 17) and the right atom layer (i.e., atoms of 3, 4, 5, 6, 7, 8 and 9) move towards the $[00\bar{1}]$ direction, which results in the drop of D_{4-10} correspondingly. Figure 3(e) shows the distance evolutions between atoms during the phase transformation. It can be seen that the distances between atom layers described by D_{1-4} and D_{6-17} also appears to be a modest increase from 0.410 nm to 0.465 nm owing to stretching force in [100] direction. Even in the same atom layer there are slight changes in the distances among the atoms 3, 4 and 5 (see the plots of D_{3-4} and D_{4-5}). Figure 3(f) shows the variations of angles α and β as the strain increase. It is not difficult to find that angles α and β change from 110 degree and 125 degree in the bcc lattice respectively into identical 120 degree in hcp lattice. When the phase transformation completes, the (110) plane of bcc lattice in Figure 3(a) transits into the (0001) plane of hcp lattice in the Figure 3(b).

Based on the results above, we can conclude that the phase transformation process shown in Figure 3 is fully corresponding to the Burgers mechanism proposed by

Dmitriev [47, 49]. At $\varepsilon = 15.2\%$, the value of D_{1-4} is 0.4174 nm, the D_{3-4} is 0.2558 nm, and the D_{1-4} / D_{3-4} is 1.63 (exactly the ideal axial ratio c/a of hcp lattice) as well as the angles of α and β completely evolve into 120 degree. Therefore these observations reflect an interesting fact that the bcc structure of Cu film has transitioned completely into a perfect hcp structure at $\varepsilon = 15.2\%$. Such results presented here are more precise than those reported by Jona et al. [25] who used first-principles total-energy method to calculate the lattice parameters of hcp Cu film growing epitaxially on a W{001} substrate.

The fact that this fcc \rightarrow bcc \rightarrow hcp successive phase transformation of Cu film under tensile stress is never observed previously may be due to the rather strict formation conditions. To determine the conditions for fcc \rightarrow bcc \rightarrow hcp phase transformation, a series of MD simulations under different parameters, including tensile direction, tensile speed, film thickness, simulation temperature, and relax time, are carried out. The percentages of atoms with bcc structure and hcp structure formed during the stretching process are plotted as a function of the strain. It is noted that orthogonal experimental method is used for the simulation parameters, i.e., only a single parameter changes while others keep constant during stretching process.

Figure 4 describes the percentages of atoms with bcc structure (Figure. 4(a)) and hcp structure (Figure. 4(b)) under different tensile direction. In the case of [100] tensile direction, the percentages of atoms with bcc structure and hcp structure can reach 100% when the strain $\varepsilon = 10\% \sim 14\%$ and $\varepsilon = 14\% \sim 32\%$, respectively, as discussed above. For the [110] tensile direction, however, the atoms with bcc structure only account for about 65% at $\varepsilon = 16\%$, and the percentage of hcp structure reaches 95% at $\varepsilon = 20\%$. For the [111] tensile direction, the case is worse because there are few bcc atoms formed and the hcp atoms only account for 50% when $\varepsilon = 10\% \sim 15\%$. These observations suggest that during stretching deformation along [110] and [111] direction the phase transformations are not thorough and complete. This result is fully consistent with Neogi's simulation investigation on shock-induced phase transformations of single crystal copper [28, 29].

The dependence of formation of bcc and hcp structure on the tensile speed is shown in Figure 5. To examine the influence of tensile speed, tensile speed is set within a wide range from $1 \times 10^8/s$ to $1 \times 10^{11}/s$. Seen from Figure 5(a), fcc Cu can transit into bcc Cu completely in the considered range of tensile speed, however the existence time of bcc structure will be variable. As the tensile speed increases, the existence time of bcc structure will be extended. Figure 5(b), which displays the percentages of atoms with hcp structure forming under the different tensile speed, suggests that only tensile speed $1 \times 10^{10}/s$ can make it possible to form 100% hcp Cu. That is to say, the optimum tensile speed for thorough phase transformation of bcc \rightarrow hcp is a unique value rather than a range. To explore the mechanisms for this confusing behavior, the stress-strain plots under the different tensile speeds were observed. We found that compared with other tensile speed, the stress value in case of tensile speed of $1 \times 10^{10}/s$ was maximum at the strain $\varepsilon = 14.2\%$, where phase transformation from bcc to hcp began to take place. The detailed mechanism remains unsettled at present, which calls for a further study in future.

Several studies had proved that size effects, such as size, shape, or aspect ratio, have a great influence on the mechanical properties and deformation mechanism of nano-scale materials[52-55]. For instance, P. Rohith et al.[56] implemented molecular dynamics (MD) simulations to investigate the influence of aspect ratio on tensile deformation of [100] Cu nanowires. The simulation results indicated that the Young's modulus and yield strength have been sensitive mainly to nanowire cross-section width and remains independent of nanowire length. In order to examine the dependence of phase transformation on the film's thickness h , five different thicknesses, namely $h = 0.7230$ nm, 1.0850 nm, 2.169 nm, 4.338 nm and 18.08 nm, respectively, are considered to examine the formation of bcc and hcp structure, as shown in Figure 6. Seen from Figure 6(a), the thickness of Cu film have no effect on the formation of bcc structure except that the existence time of bcc structure is slightly short in the case of thicker film. For the hcp structure, too thick ($h \geq 18.08$ nm) or too

thin ($h \leq 0.7230$ nm) film is unfavorable to the formation of hcp lattice structure as it only makes 90% atoms transit into the hcp structure (see Figure 6(b)).

The plots in Figure 7 depict the dependence of formation of bcc and hcp structure on the temperature. As is shown in Figure 7(a), high temperatures will lead to the short existence time of bcc structure. This probably arises from the thermal activation induced by high temperature, which destroys the regular configuration of atoms in the film. Such an impact of high temperature appears to be more notable for the formation of hcp structure. We have found that only when the temperature $T \leq 10$ K, the whole Cu film can transit completely from bcc structure into hcp structure (see Figure 7(b)).

In the present work, the uniaxial tension simulation is continuous without any relax procedure during stretching process, which is the same as the “continuous straining” mode described by Komanduri et al.[57] and Wang et al.[58]. On the other hand, some MD simulations on the tensile test of metallic film adopted quasistatic stretching[4, 5, 6], namely, the relax procedure is performed for a period of time after a part of stretching has been completed. To explore the influence of relax time on the formation of bcc and hcp structure, we carry out tensile simulations with different relax time. During the process of tension simulation, the bcc structure of Cu can form in the case of existence of relaxation procedure, but the existence time of bcc structure becomes more and more short with the relax time increasing (see Figure 8(a)). As for the bcc→hcp, the relax procedure has a greater impact on the hcp formation. Figure 8(b) shows that even the relax time of 0.05 ps makes the transformation of hcp structure be incomplete. The relaxation procedure during stretching process, as is known, will reduce the internal stress in thin film. Thus the phenomenon shown in Figure 8 indicates that reduction in stress induced by relaxation procedure is unfavorable to the occurrence of phase transformation.

3 Conclusions

MD simulation has been performed to study the uniaxial tensile process of ultrathin Cu film along the [100] direction. It is discovered that with the increasing stress, the Cu film undergoes a successive phase transformations of fcc→bcc→hcp. Moreover,

the phase transformation process is very fast and thorough, i.e., all parents phase can transit into the new phase almost instantaneously. Such novel phenomenon has never observed in the previous MD simulation studies on the deformation of metallic thin films. The tracer atoms analysis is used to explore the crystallography mechanisms of two phase transformations, which indicates that the two phase transformation are fully corresponding to Bain and Burgers mechanism, respectively. For the fcc→bcc transformation, the formed bcc structure has a lattice constant of 0.286 nm at the strain $\varepsilon = 12.4\%$, and for the bcc→hcp transformation, the formed hcp structure has an axial ratio of 1.63 at the strain $\varepsilon = 15.2\%$. Those interesting results indicate that the simulation system used in our study is distinctive, which provides an ideal model for investigating the exact path of martensitic phase transformation in Cu film and determining the decisive factors in forming these higher-energy phases. We examine the formation conditions of fcc→bcc→hcp successive phase transformations in Cu film, revealing that it can only occur under the strict simulation conditions, namely stretching along [100] (or [010], [001]) direction, definitive tensile speed ($1 \times 10^{10}/s$), appropriate film thickness ($0.7230 \text{ nm} \leq h \leq 18.08 \text{ nm}$), low simulation temperature ($T \leq 10\text{K}$), and continuous stretching process without any relaxation procedure.

References

- [1] K. Bhattacharya and R. D. James, *Science* 307(2005): 53-54
- [2] J.M. Falkowski, and Y. Surendranath, *Acs Catalysis* 5(2016): 150421134344006
- [3] W.S. Lai, and X.S. Zhao, *Appl. Phys. Lett.* 85(2004): 4340-4342
- [4] Q.N. Guo, X.D. Yue, S.E. Yang, and Y.P. Huo, *Comput. Mater. Sci.* 50(2010): 319-330
- [5] S. Xu, Y.F. Guo, and Z.D. Wang, *Comput. Mater. Sci.*, 67(2013): 140-145
- [6] J. Wang, W. Hu, X. Li, S. Xiao, and H. Deng, *Comput. Mater. Sci.* 50(2013): 373-377
- [7] P.S. Branício, and J.Rino, *Phys. Rev. B* 62(2000): 16950-16955
- [8] F. Milstein and S. Chantasiriwan, *Phys. Rev. B* 58(1998): 6006-6018
- [9] H.K.D.H. Bhadeshia, *Encyclopedia of Materials Science: Science and Technology*, edited by K. H. J. Buschow, et al., Elsevier Science, New York, 2001, p. 5203
- [10] G.B. Olson and W. Owen, *Martensite. A Tribute to Morris Cohen*, ASM International, Materials Park, OH, 1992
- [11] D. Bancroft, E.L. Peterson, and S. Minshall. *J. Appl. Phys.* 27 (1956):291-298
- [12] H. Fujiwara, H. Inomoto, R. Sanada, and K. Ameyama. *Scripta Mater.* 44 (2001): 2039-2042
- [13] J. Zhang, and F. Guyot. *Phys. Chem. Minerals* 26 (1999): 419-424
- [14] J. Ivanisenko, I. MacLaren, X. Sauvage, R. Valiev, and H.J. Fecht. *Solid State Phen.*114 (2006): 133-144
- [15] H. Li, S.C. Wu, D. Tian, J. Quinn, Y. S. Li, F. Jona, and P. M. Marcus, *Phys. Rev. B* 40 (1989): 5841-5844.
- [16] H. Li, S.C. Wu, J. Quinn, Y.S. Li, D. Tian, and F. Jona, *J. Phys. Condensed Matter.* 3 (1991): 7193-7198.
- [17] H. Li, D. Tian, J. Quinn, Y.S. Li, F. Jona, and P. M. Marcus, *Phys. Rev. B* 43 (1991): 6342-6346.
- [18] Z.Q. Wang, S.H. Lu, Y.S. Li, F. Jona, and P. M. Marcus, *Phys. Rev. B* 35 (1987): 9322-9325.

- [19] I.A. Morrison, M.H. Kang, and E.J. Mele, *Phys. Rev. B* 39 (1989): 1575-1580.
- [20] H. Kung, Y.C. Lu, A.J. Griffin Jr., M. Nastasi, T.E. Mitchell, and J.D. Embury, *Appl. Phys. Lett.* 71 (1997): 2103-2105.
- [21] T.E. Mitchell, Y.C. Lu, A.J. Griffin Jr., M. Nastasi, H.Kung, *J. Am. Ceram. Soc.* 80 (1997):1673-1676
- [22] P. M. Marcus, F. Jona, and S. L. Qiu, *Phys. Rev. B* 66 (2002): 064111.
- [23] Y. Mishin, M. J. Mehl and D. A. Papaconstantopoulos, A. F. Voter and J. D. Kress, *Phys. Rev. B* 63 (2001):224106.
- [24] L.G. Wang and M. Sob, *Phys. Rev. B* 60 (1999): 844-851.
- [25] F. Jona, X. Z. Ji, and P. M. Marcus, *Phys. Rev. B* 68 (2003): 172101.
- [26] K. Kolluri, M.R. Gungor, and D. Maroudas, *Phys. Rev. B* 78(2008): 195408
- [27] S. Tang, J.C. Wang, B. Svendsen, and D. Raabe, *Acta Materialia*, 139(2017): 196-204
- [28] A. Neogi and N. Mitra, *American Institute of Physics Conference Series*, 1832(2017): 317-319
- [29] A. Neogi and N. Mitra, *Scientific Reports*, 7(1)(2017): 7337
- [30] S. Melchionna, G. Ciccotti, and B.L. Holian, *Mol. Phys.* 78 (1993): 533-544.
- [31] M. Zhou, *Proc. Royal Soc. London A.* 459(2003): 2347
- [32] M.A. Tschopp, D.E. Spearot, and D.L. McDowell, *Model. Simul. Mater. Sci. Eng.* 15(2007): 693-709
- [33] M.A. Tschopp, and D.L. McDowell, *J. Mech. Phys. Solids* 56(2008): 1806-1830
- [34] S. Plimpton, *J. Comput. Phys.*, 117(1)(1995): 1-9
- [35] J. A. Zimmerman, H. Gao, and F. F. Abraham, *Modell. Simul. Mater. Sci. Eng.* 8(2000): 103-115
- [36] A. Stukowski, *Modell. Simul. Mater. Sci. Eng.* 18 (2010): 015012
- [37] J.D. Honeycutt and H.C. Andersen, *J. Phys. Chem.* 90 (1986): 1585-1589
- [38] Z.K. Lu, and G.J. Weng, *Journal of the Mechanics & Physics of Solids*, 45(1997):1905-1921
- [39] R.F. Hamilton, C. Efstathiou,, H. Sehitoglu, and Y. Chumlyakov, *Scripta Mater.* 54 (2006): 465–46

- [40] F. Milstein and B. Farber, *Phys. Rev. Lett.* 44(1980): 277-280
- [41] G. Grimval, B.M. Kope, V. Ozolins, and K.A. Persson, *Rev. Mod. Phys.* 84(2012): 945
- [42] Y.F. Wen, and J. Sun, *Comput. Mater. Sci.* 79 (2013): 463-467
- [43] M. Jahnatek, J. Hafner, and M. Krajci, *Phys. Rev. B* 79 (2009): 224103.
- [44] F. Jona and P. M. Marcus, *Phys. Rev. B* 63 (2001): 094113.
- [45] H. Djohari, F. Milstein, and D. Maroudas, *Phys. Rev. B* 79 (2009): 174109
- [46] F. Milstein, J. Marschall, and H.E. Fang, *Phys. Rev. Lett.* 74(1995): 2977-2980
- [47] V.P. Dmitriev, Y.M. Gufan, and P. Tolédano, *Phys. Rev. B* 44 (1991): 7248-7256
- [48] E.C. Bain, *Trans AIME*, 70(1924): 25-35
- [49] W.G. Burgers, *Physica*, 1(1934): 561-586
- [50] Z. Tang, M. Hasegawa, Y. Nagai and M. Saito, *Phys. Rev. B* 65 (2002): 195108.
- [51] Y. Zhou, W. Lai and J. Wang, *Phys. Rev. B* 49 (1993): 4463-4467.
- [52] M. Yaghoobi, G.Z. Voyiadjis, *Acta Mater.* 121(2016): 190–201
- [53] Z. Wu, Y.W. Zhang, M.H. Jhon, H. Gao, D.J. Srolovitz, *Nano Lett.* 12(2012): 910–914
- [54] J. Han, L. Fang, J. Sun, Y. Han, K. Sun, *J. Appl. Phys.* 112(2012): 114314
- [55] H. Liang, M. Upmanyu, H. Huang, *Phys. Rev. B* 71(2005): 241403
- [56] P. Rohith, G. Sainath, B.K. Choudhary, *Comput. Mater. Sci.* 138(2017): 34-41
- [57] R. Komanduri, N. Chandrasekaran, and L.M. Raff, *Mater. Sci. Eng. A* 340(2003): 58-67
- [58] D. X. Wang, J.W. Zhao, S. Hu, X. Yin, S. Liang, Y.H. Liu, and S.Y. Deng, *Nano Lett.* 7 (2007): 1208-1212

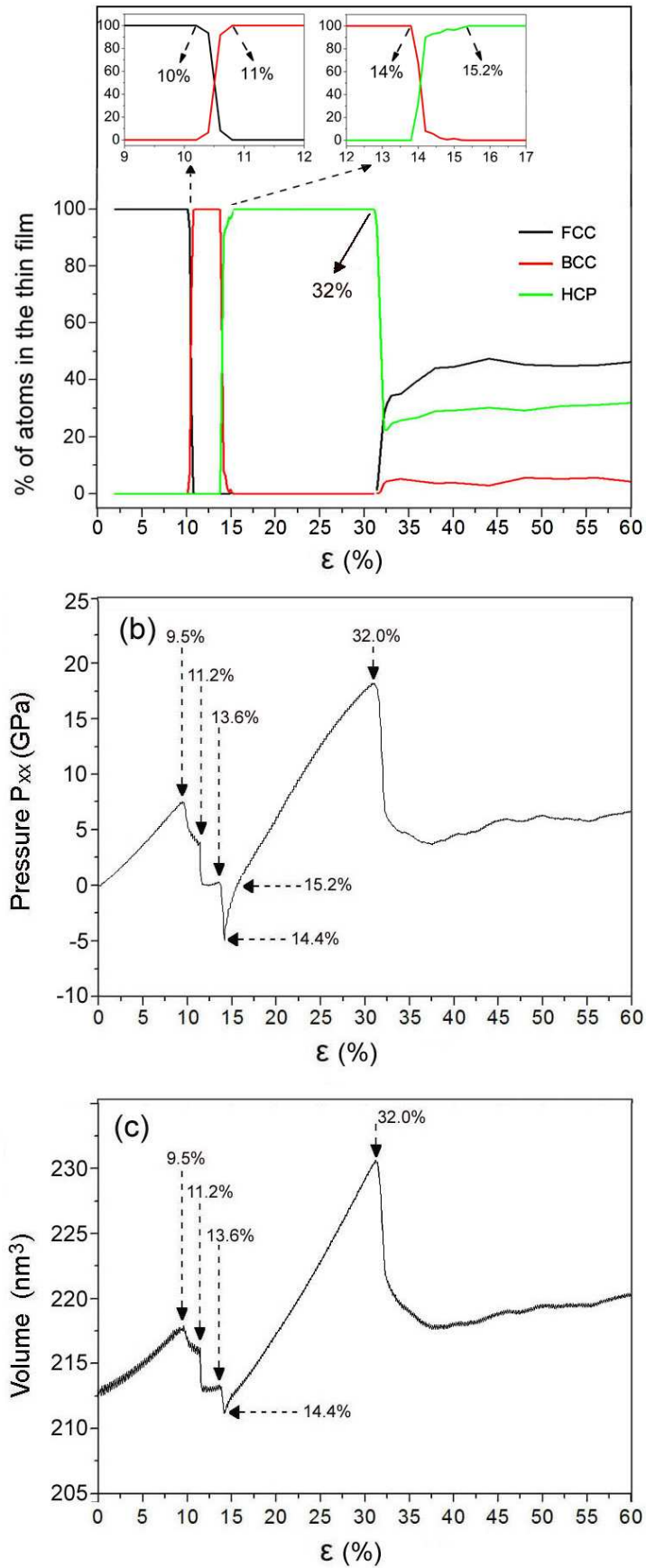


Figure 1 Process of uniaxial tensile of ultrathin (1.08 nm) Cu film. The continuous MD simulation without any relax procedure is performed in the isobaric-isothermal(*NPT*) ensemble with the temperature of 10K, the tensile direction of [100], and the tensile speed of 1×10^{10} /s. (a) Variation of percentage of different lattice structures where the black, red and green lines stand for fcc, bcc and hcp structures, respectively. The two insets show the variations of percentages of different lattice structures in details. The one at the top left corner presents the variations of fcc and bcc lattice structures, and the other one at the top right corner presents the variations of bcc and hcp lattice structures. (b) Variation of the pressure in the *x* direction. (c) Variation of the volume of the Cu film.

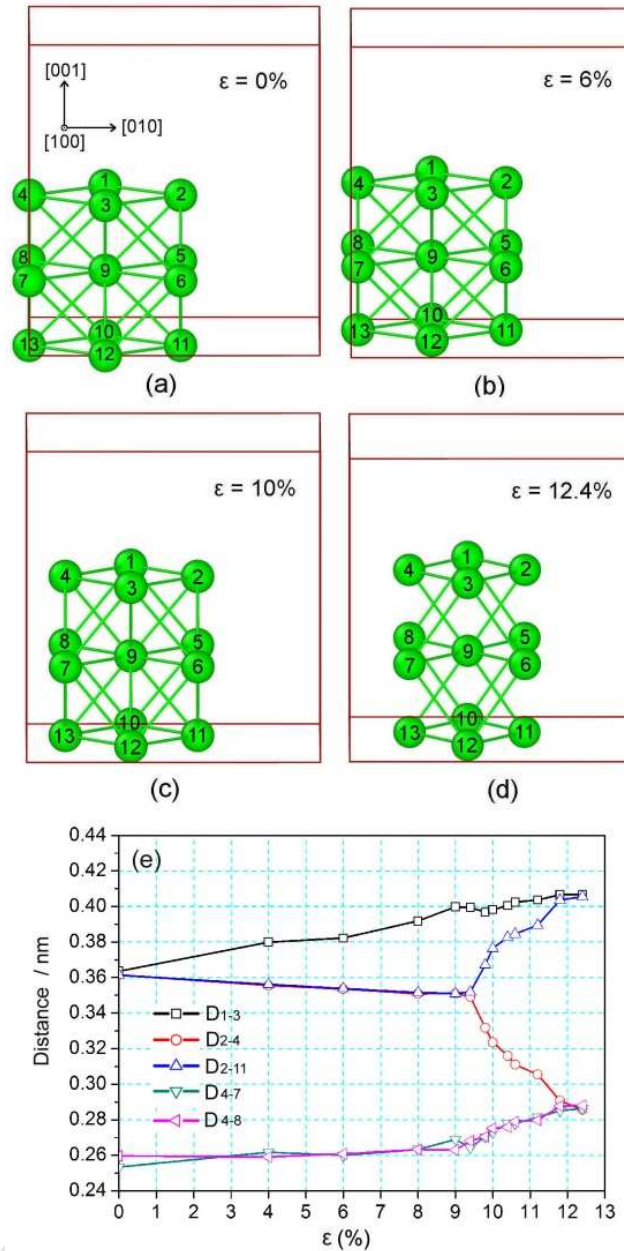


Figure 2 (a) - (d) Snapshots of tracer atoms showing the phase transformation of fcc \rightarrow bcc. To show the movement of tracer atoms clearly, a virtual simulation box is added. From (a) to (d), the strain applied on the Cu film is 0%, 6%, 10% and 12.4%, respectively; (e) Evolution of the distance between atoms as the strain increases from 0% to 12.4%.

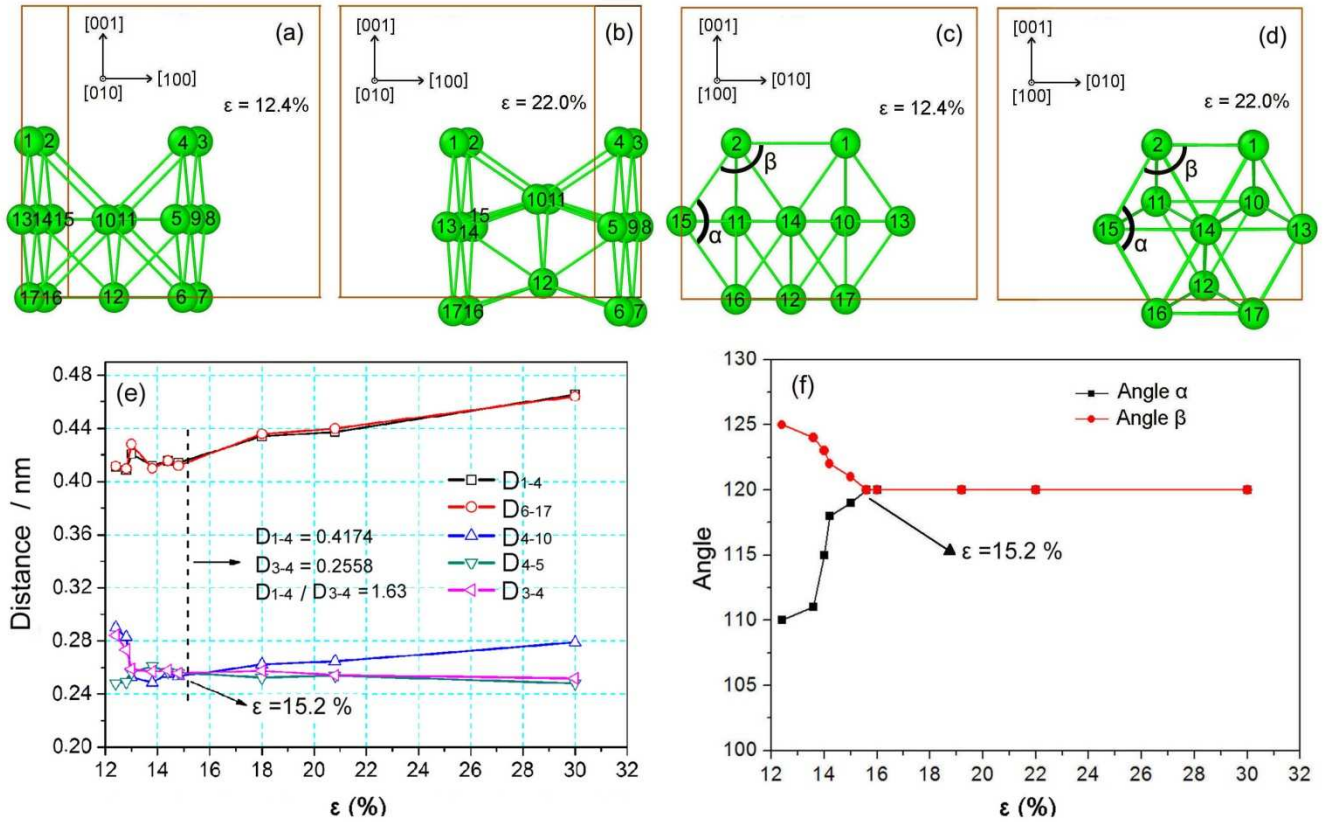


Figure 3 (a) - (d) Snapshots of tracer atoms showing the phase transformation of bcc→hcp. (a) View from [010] direction, and the strain $\varepsilon = 12.4\%$; (b) View from [010] direction, and the strain $\varepsilon = 22.0\%$; (c) View from [100] direction, and the strain $\varepsilon = 12.4\%$; (d) View from [100] direction, and the strain $\varepsilon = 22.0\%$; (e) Evolution of the distance between atoms as the strain increases from 12.4% to 30.0%; (f) Evolution of the angles α and β as the strain increases from 12.4% to 30.0%.

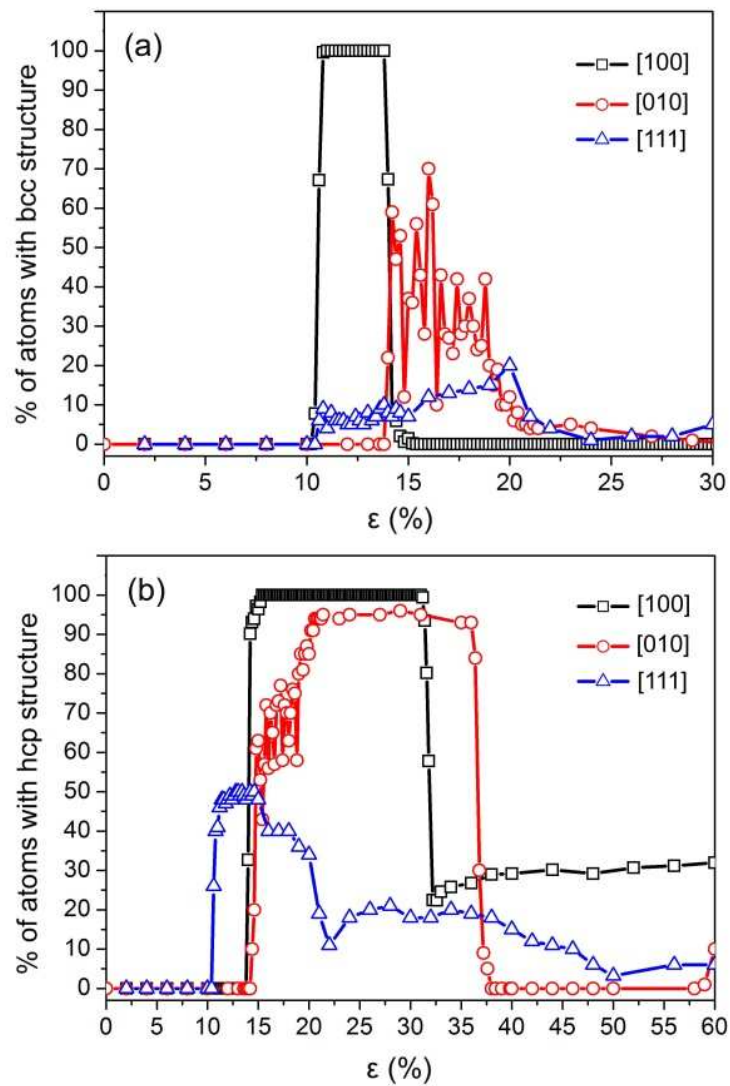


Figure 4 Variation of percentage of atoms with different structures as the applied tensile strain ϵ increases. (a) Bcc structure; (b) Hcp structure. The black, red and blue lines stand for the tensile direction of [100], [110] and [111], respectively.

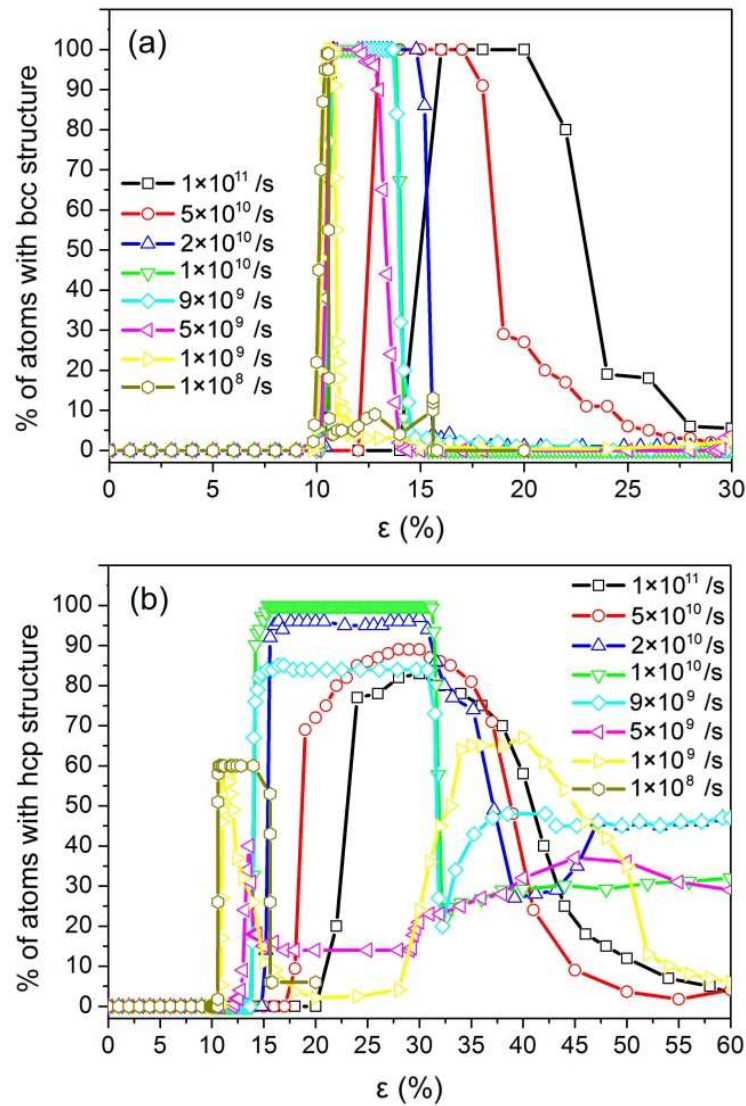


Figure 5 Variation of percentage of atoms with different structures under different tensile speeds as the applied tensile strain ϵ increases. (a) Bcc structure; (b) Hcp structure. The black, red, blue, green, cyan, magenta, yellow, and dark yellow lines stand for the tensile speed of 1×10^{11} /s, 5×10^{10} /s, 2×10^{10} /s, 1×10^{10} /s, 9×10^9 /s, 5×10^9 /s, 1×10^9 /s, 1×10^8 /s, respectively.

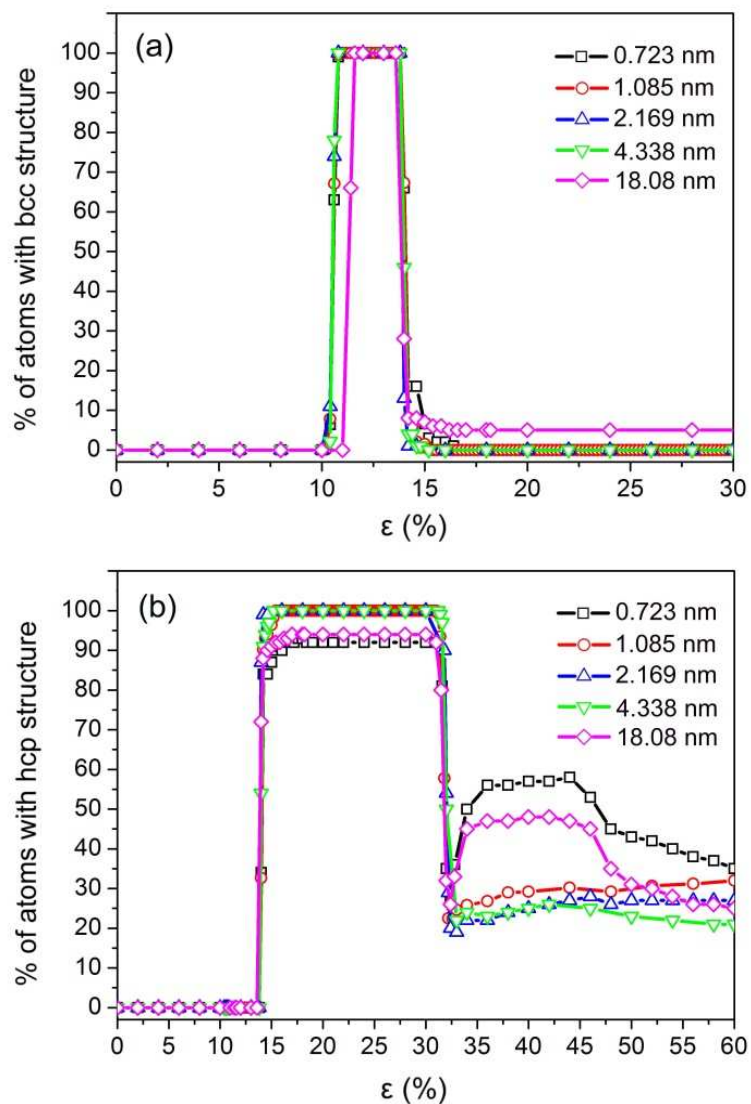


Figure 6 Variation of percentage of atoms with different structures in the Cu film with different thicknesses as the applied tensile strain ϵ increases. (a) Bcc structure; (b) Hcp structure. The black, red, blue, green and magenta lines stand for the film's thicknesses of 0.7230 nm, 1.085 nm, 2.169 nm, 4.338 nm and 18.08 nm, respectively.

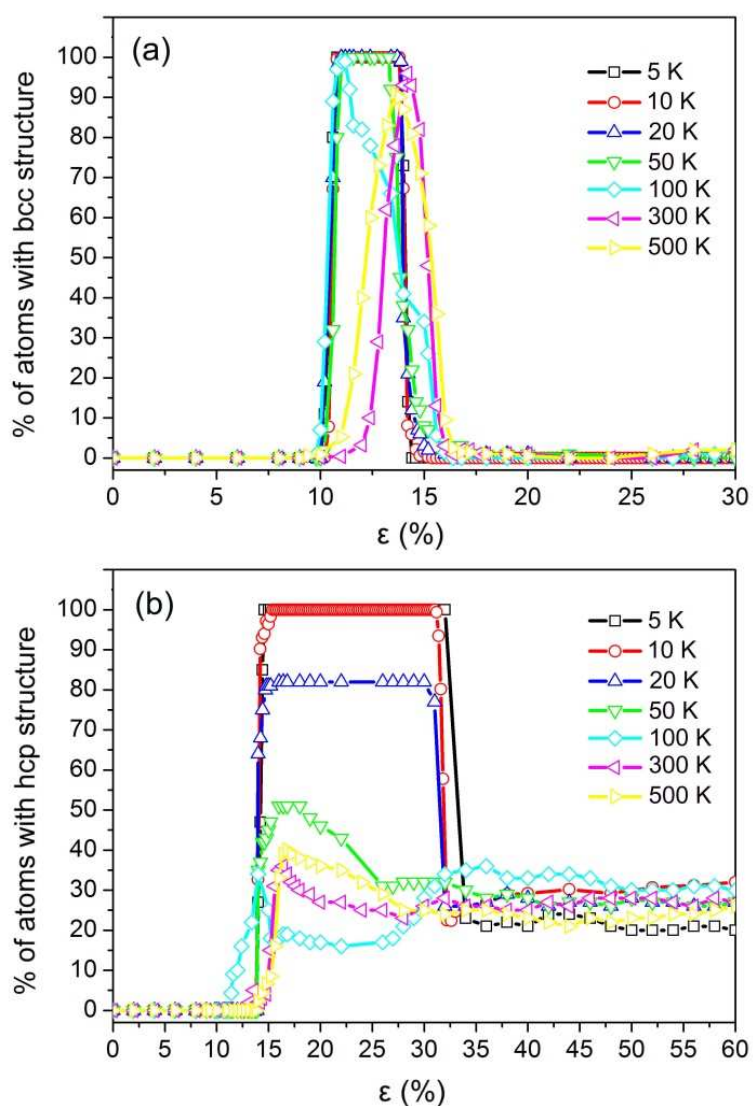


Figure 7 Variation of percentage of atoms with different structures under different temperatures as the applied tensile strain ϵ increases. (a) Bcc structure; (b) Hcp structure. The black, red, blue, green, cyan, magenta, and yellow lines stand for the temperatures of 5K, 10K, 20K, 50K, 100K, 300K and 500K, respectively.

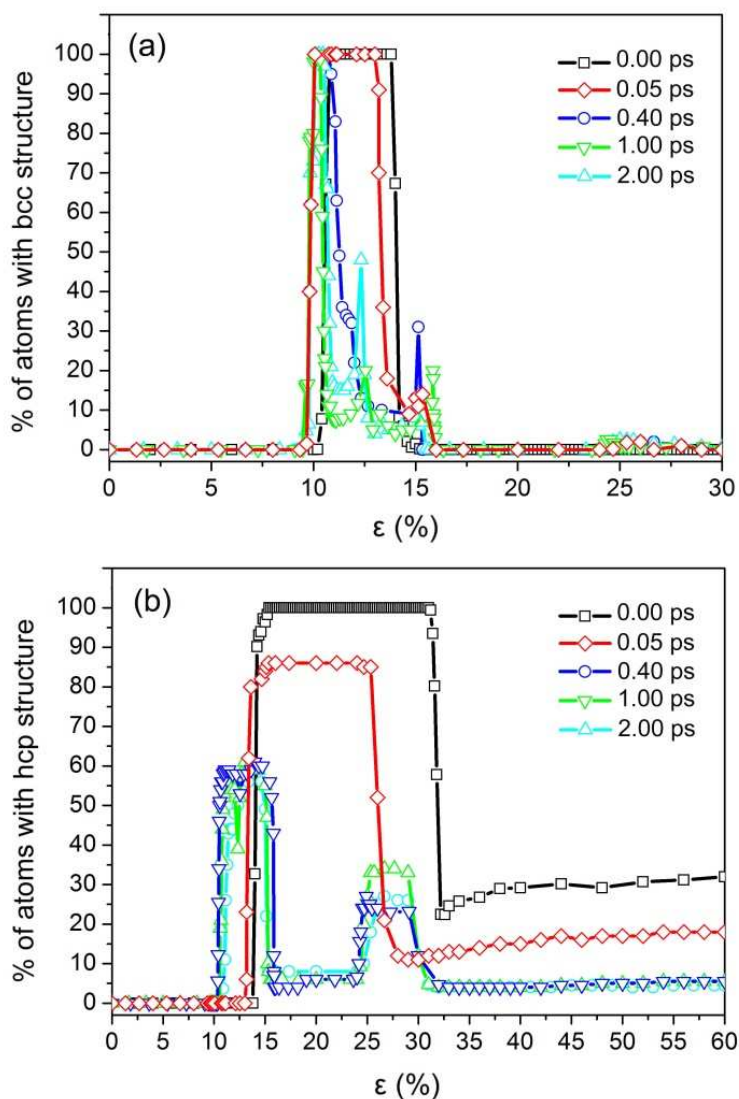


Figure 8 Variation of percentage of atoms with different structures as the applied tensile strain ϵ increases. (a) Bcc structure; (b) Hcp structure. The black, red, blue, green, and cyan lines stand for the relax time of 0.00ps, 0.05ps, 0.40ps, 1.00ps, 2.00ps, respectively.

- 1) A $\text{fcc} \rightarrow \text{bcc} \rightarrow \text{hcp}$ successive phase transformations are discovered during the Cu film stretching.
- 2) Very fast and thorough phase transformation process.
- 3) The two phase transformations are consist with Bain and Burgers mechanisms.
- 4) The successive phase transformations occur only under very strict conditions.